



Published in final edited form as:

*Inorg Chem.* 2023 August 14; 62(32): 12630–12633. doi:10.1021/acs.inorgchem.3c02163.

## Coordination chemistry controls coenzyme B<sub>12</sub> synthesis by human ATP:cob(I)alamin adenosyltransferase

Harsha Gouda,

Zhu Li,

Markus Ruetz,

Ruma Banerjee\*

Department of Biological Chemistry, University of Michigan, Ann Arbor, MI 48109 USA

### Abstract

Cobalamin (or vitamin B<sub>12</sub>)-dependent enzymes and trafficking chaperones exploit redox-linked coordination chemistry to control cofactor reactivity during catalysis and translocation. As the cobalt oxidation state decreases from 3+ to 1+, the preferred cobalamin geometry changes from 6- to 4-coordinate. In this study, we reveal the sizeable thermodynamic gain that accrues for human ATP:cob(I)alamin adenosyltransferase (or MMAB) by enforcing an unfavorable 4-coordinate cob(II)alamin geometry. MMAB-bound cob(II)alamin is reduced to the supernucleophilic cob(I)alamin intermediate during synthesis of 5'-deoxyadenosylcobalamin. Herein, we report the first experimentally determined reduction potential for 4-coordinate cob(II)alamin ( $-325 \pm 9$  mV), which is 180 mV more positive than for the 5-coordinate water-liganded species. The redox potential of MMAB-cob(II)alamin is within range of adrenodoxin, which we demonstrate functions as an electron donor. We also show that stabilization of 5-coordinate cob(II)alamin by a subset of MMAB patient variants, compromises reduction by adrenodoxin, explaining the underlying pathogenic mechanism.

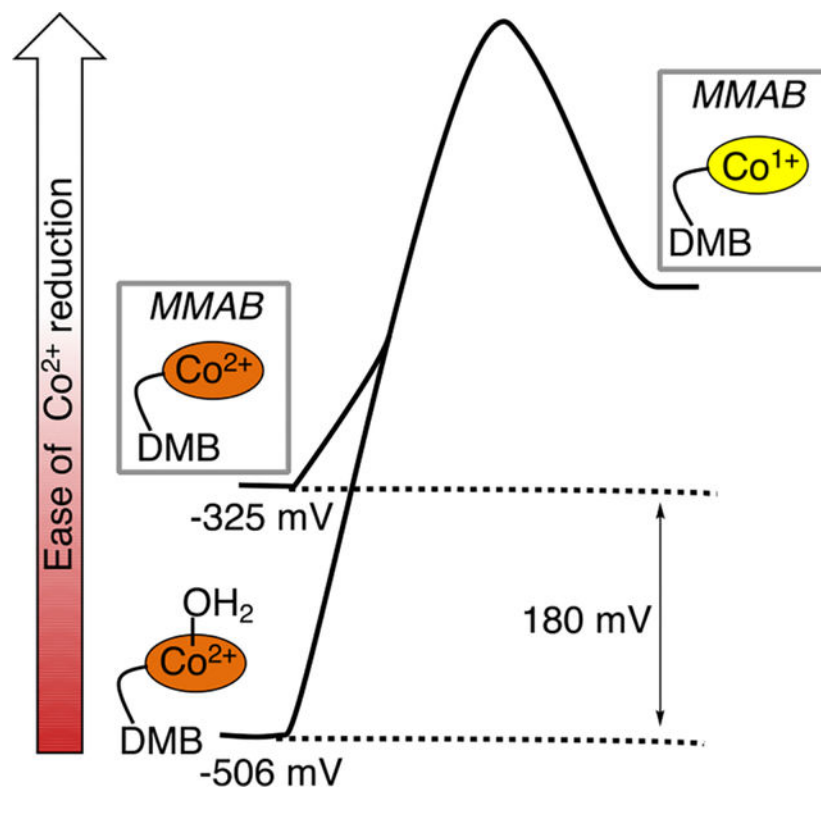
### Graphical Abstract

---

\*Corresponding author: rbanerje@umich.edu.

Supporting Information Available

Materials and Methods, Figures S1–S4 and references are available in the Supporting Information section.



## Introduction

5'-deoxyadenosyl cobalamin (AdoCbl) serves as a radical-generator for B<sub>12</sub>-dependent enzymes that catalyze 1,2 rearrangement reactions<sup>1</sup>. Methylmalonyl-CoA mutase (MMUT), the only AdoCbl-dependent enzyme found in humans, catalyzes the isomerisation of (*R*)-methylmalonyl-CoA to succinyl-CoA and serves an anaplerotic function<sup>2</sup>. Following cellular entry, B<sub>12</sub> is processed, assimilated, and escorted to MMUT via an elaborate trafficking pathway<sup>3</sup>. In the mitochondrial matrix, inactive cob(II)alamin is converted to the active AdoCbl form by ATP:cob(I)alamin adenosyltransferase (or MMAB for methylmalonic aciduria type B)<sup>4,5</sup> (Fig. 1A). MMAB also doubles as an escort and delivers AdoCbl to MMUT<sup>6,7</sup>, a radical enzyme<sup>8</sup>. In the absence of apo-MMUT, MMAB sacrifices AdoCbl via cobalt-carbon bond homolysis, as a strategy to sequester cob(II)alamin, which is bound more tightly than AdoCbl<sup>9</sup> (Fig. 1A). Mutations in MMAB can impair cofactor synthesis, delivery and/or sequestration<sup>9-11</sup>, leading to loss of MMUT function and methylmalonic aciduria, an inborn error of metabolism<sup>12</sup>. MMAB also serves as a repair enzyme, accepting inactive cofactor that is occasionally generated on MMUT during catalytic turnover, in a process that requires a G-protein chaperone, MMAA<sup>13</sup>.

The B<sub>12</sub> binding pocket in MMAB is fully organized upon ATP binding, which leads to ordering of a mobile N-terminal loop<sup>14</sup>. Cob(II)alamin binds in the “base-off” state<sup>6,15</sup> where the lower axial dimethylbenzimidazole (DMB) ligand to the cobalt ion in solution, is displaced by the non-coordinating Phe-170 (Fig. 1B). The active site of MMAB is sealed off from solvent access, which precludes water coordination to the cobalt ion and stabilizes

4-coordinate (4-c) cob(II)alamin, characterized by a 464 nm absorbance peak versus 472 nm, associated with 5-c cob(II)alamin (Fig. 1C). The preferred coordination number for cobalamin is inversely correlated with redox and decreases from 6- to 5- to 4-c as the cobalt is reduced from the 3+ to 2+ to 1+ oxidation state<sup>16</sup>. The MMAB reaction requires the one-electron reduction of cob(II)alamin to cob(I)alamin, followed by nucleophilic displacement of the adenosyl moiety of ATP, generating AdoCbl and triphosphate (PPPi) (Fig. 1A). Computational studies predict an ~250 mV gain in the redox potential by stabilization of 4-c cob(II)alamin<sup>17</sup>. The predicted shift in the redox potential from -506 mV<sup>18</sup> to >-350 mV<sup>17</sup> (versus the standard hydrogen electrode) for 5- versus 4-c base-off cob(II)alamin/cob(I)alamin, would bring it within range of biological reductases. Other adenosyltransferases also stabilize square planar cob(II)alamin<sup>19</sup>. However, experimental determination of the redox potential has been challenging, since cob(II)alamin binding to adenosyltransferases requires ATP, which in turn reacts very rapidly with cob(I)alamin and precludes establishment of a redox equilibrium. To circumvent this limitation, we tested AMP and ADP as potential ATP mimics to promote cob(II)alamin binding but prevent reaction with cob(I)alamin. Surprisingly, ADP served as an alternate substrate, forming AdoCbl, but supported only a single turnover while AMP did not promote cob(II)alamin binding (Fig. S1).

Next, we turned to the disease-causing variant R190H, which decreases  $k_{\text{cat}}$  110-fold relative to wild-type human MMAB in the presence of the strong reductant, titanium(III)citrate<sup>10</sup>. Arg-190 makes multiple electrostatic contacts with ATP on both sides of the scissile bond (Fig 1D). Significantly, in contrast to wild-type MMAB, cob(I)alamin accumulation is observed with the R190H variant in the presence of titanium(III)citrate and ADP (Fig 2A), supporting the feasibility of using this variant for measuring the cob(II)alamin/cob(I)alamin redox potential. Square planar coordination of cob(II)alamin bound to R190H MMAB was confirmed by electron paramagnetic resonance (EPR) spectroscopy, which allows ready distinction between 4- and 5-c cob(II)alamin with an axial water ligand (Fig 2B). Importantly, the EPR spectra of cob(II)alamin bound to wild-type and R190H MMAB were comparable, ruling out significant perturbations in the environment around the metal ion.

Spectroelectrochemical titrations were performed with benzyl viologen ( $E^0 = -359$  mV) and the ratio of reduced to oxidized benzyl viologen and cob(II)alamin was determined using the isosbestic point at 524 nm ( $BV_{\text{ox}}/BV_{\text{red}}$ ) and 464 nm (cob(II)alamin/cob(I)alamin) (Fig 2C). Nernst analysis yielded a straight line with a slope of  $0.91 \pm 0.1$  ( $n=4$ ), consistent with a one-electron transfer, and provided the first experimental estimate of the redox potential for 4-c cob(II)alamin of  $-325 \pm 9$  mV (Fig 2C, *inset*). At the end of the titration, HPLC analysis was used to assess whether reaction of cob(I)alamin with ADP, forming AdoCbl, had occurred during the ~15 min needed to complete the titration. AdoCbl was not detected while aquocobalamin ( $H_2OCbl$ ), formed by the oxidation of cob(II)alamin and cob(I)alamin, was the predominant peak (Fig 2D). The smaller peak at 14.3 min which was also present in the  $OH_2Cbl$  (13.6 min) standard, had an absorption spectrum identical to it, and increased in intensity from 10 to 22% over the course of the titration (Fig S4).

AdoCbl synthesis by the *Brucella melitensis* and *Salmonella enterica* adenosyltransferases<sup>20, 21</sup> is supported by the NADH-dependent flavoprotein, cobalamin

reductase. In vitro, human methionine synthase reductase can deliver electrons for AdoCbl synthesis<sup>4</sup>, revealing the feasibility of flavoproteins with a redox potential in the  $-220$  mV range<sup>22</sup>, to couple to human MMAB. However, methionine synthase reductase is a cytoplasmic protein and its deficiency is not known to impair mitochondrial cobalamin metabolism<sup>23</sup>.

Clinical genetics studies have failed to identify a mitochondrial reductase associated with inherited cobalamin disorders, indicating that the MMAB redox partner is likely to be shared with other electron acceptors. We therefore examined the ability of adrenodoxin, (FDX1), a [2Fe-2S]-containing mitochondrial reductase, with a redox potential of  $-267 \pm 5$  mV<sup>20</sup>, to serve as an electron donor to MMAB in the presence of ferredoxin reductase (FDXR) and NADPH<sup>24</sup>. FDX1 is important for heme and lipoyl cofactor synthesis as well as steroidogenesis<sup>25</sup>. Recombinant human FDX1 can support MMAB-dependent biosynthesis of AdoCbl from cob(II)alamin (Fig 3A). The NADPH-driven synthesis of AdoCbl in the presence of FDX1/FDXR ( $k_{\text{cat}} = 4.7 \pm 0.5 \text{ min}^{-1}$ ) is 2.5-fold lower than in the presence of titanium(III)citrate ( $11.5 \pm 1.5 \text{ min}^{-1}$ ). The time-dependent spectral changes observed in the steady-state assay, correspond to the MMAB-catalyzed conversion of base-on 5-c cob(II)alamin (474 nm) to base-on 6-c AdoCbl (522 nm) and its release into solution (Fig 3A). Michaelis-Menten kinetic analysis yielded a  $K_M$  for reduced FDX1 of  $135 \pm 24$  nM (Fig 3A, *inset*). A stable complex between oxidized FDX1 and MMAB was not observed by size exclusion chromatography, suggesting that a transient complex is formed between them for electron transfer. In the absence of either FDX1 or FDXR, AdoCbl synthesis by MMAB is not observed.

Next, the efficacy of FDX1-dependent AdoCbl synthesis was assessed with clinical variants of MMAB including R190H/C, E193K, and R186Q (Fig. 3B). Unlike the wild-type enzyme, E193K MMAB binds cob(II)alamin in a 5-c state with an axial water ligand<sup>9, 10</sup> while R186Q MMAB binds “base-on” 5-c cob(II)alamin i.e. with a lower axial DMB ligand<sup>9</sup>. In the presence of titanium(III)citrate, the activities of R186Q and E193K MMAB are comparable to wild-type enzyme but are 115- and 16-fold lower for the R190H and R190C variants<sup>9, 10</sup>. In contrast, in the presence of the FDX1/FDXR/NADPH, the activities of the R186Q and E193K MMAB are not detectable, while the R190H and R190C variants exhibit 230- and 150-fold lower AdoCbl synthesis activity compared to wild-type MMAB (Fig. 3C). Thus, the redox penalty associated with the R186Q and E193K patient mutations is only displayed in the presence of a biologically relevant reducing system. The failure to stabilize square planar cob(II)alamin is predicted to decrease its redox potential by 180 mV and 275 mV in the R186Q (DMB-ligand) and E193K (H<sub>2</sub>O ligand) mutations, respectively. We speculate that the molecular mechanism underlying methylmalonic aciduria by the R186Q and E193K variants results at least in part, from their loss of cob(II)alamin coordination chemistry control (Fig. 3D).

In summary, the experimental determination of the redox potential for 4-c cob(II)alamin illuminates the quantitatively significant advantage of this strategy in the reductive adenosylation reaction catalyzed by MMAB. The study also identifies NADPH/FDXR-driven FDX1 as a biologically competent redox partner for human MMAB; all three proteins are mitochondrial. Impaired AdoCbl synthesis by the disease-causing E193K and R186Q

variants is masked by a strong chemical reductant, but revealed by FDX1, supporting its role as a potential MMAB redox partner.

## Supplementary Material

Refer to Web version on PubMed Central for supplementary material.

## Acknowledgements

This work was supported in part by a grant from the National Institutes of Health (DK45776).

## References

- (1). Banerjee R Radical peregrinations catalyzed by coenzyme B<sub>12</sub>-dependent enzymes. *Biochemistry* 2001, 40 (21), 6191–6198. [PubMed: 11371179] Banerjee R.; Ragsdale SW. The many faces of vitamin B<sub>12</sub>: Catalysis by cobalamin-dependent enzymes. *Ann. Rev. Biochem.* 2003, 72, 209–247. [PubMed: 14527323]
- (2). Banerjee R; Chowdhury S Methylmalonyl-CoA mutase. In *Chemistry and Biochemistry of B<sub>12</sub>*, Banerjee R. Ed.; John Wiley and Sons, 1999; pp 707–730.
- (3). Banerjee R; Gouda H; Pillay S Redox-Linked Coordination Chemistry Directs Vitamin B<sub>12</sub> Trafficking. *Acc Chem Res* 2021, 54 (8), 2003–2013. DOI: 10.1021/acs.accounts.1c00083. [PubMed: 33797888]
- (4). Leal NA; Olteanu H; Banerjee R; Bobik TA Human ATP: Cob(I)alamin adenosyltransferase and its interaction with methionine synthase reductase. *J Biol Chem* 2004, 279 (46), 47536–47542. [PubMed: 15347655]
- (5). Leal NA; Park SD; Kima PE; Bobik TA Identification of the human and bovine ATP:Cob(I)alamin adenosyltransferase cDNAs based on complementation of a bacterial mutant. *J Biol Chem* 2003, 278 (11), 9227–9234. [PubMed: 12514191]
- (6). Yamanishi M; Labunska T; Banerjee R Mirror “base-off” conformation of coenzyme B<sub>12</sub> in human adenosyltransferase and its downstream target, methylmalonyl-CoA mutase. *J Am Chem Soc* 2005, 127, 526–527. [PubMed: 15643868]
- (7). Padovani D; Labunska T; Palfey BA; Ballou DP; Banerjee R Adenosyltransferase tailors and delivers coenzyme B<sub>12</sub>. *Nat Chem Biol* 2008, 4 (3), 194–196. DOI: nchembio.67 [pii] 10.1038/nchembio.67. [PubMed: 18264093] Padovani D.; Banerjee R. A Rotary Mechanism for Coenzyme B<sub>12</sub> Synthesis by Adenosyltransferase. *Biochemistry* 2009, 48, 5350–5357. [PubMed: 19413290]
- (8). Padmakumar R; Banerjee R Evidence from EPR spectroscopy of the participation of radical intermediates in the reaction catalyzed by methylmalonyl-CoA mutase. *J. Biol. Chem.* 1995, 270, 9295–9300. [PubMed: 7721850]
- (9). Campanello GC; Ruetz M; Dodge GJ; Gouda H; Gupta A; Twahir UT; Killian MM; Watkins D; Rosenblatt DS; Brunold TC; Warncke K; Smith JL; and Banerjee R Sacrificial Cobalt-Carbon Bond Homolysis in Coenzyme B<sub>12</sub> as a Cofactor Conservation Strategy. *J Am Chem Soc* 2018, 140 (41), 13205–13208. DOI: 10.1021/jacs.8b08659. [PubMed: 30282455]
- (10). Gouda H; Mascarenhas R; Pillay S; Ruetz M; Koutmos M; Banerjee R Patient mutations in human ATP:cob(I)alamin adenosyltransferase differentially affect its catalytic versus chaperone functions. *J Biol Chem* 2021, 297 (6), 101373. DOI: 10.1016/j.jbc.2021.101373. [PubMed: 34757128]
- (11). Lofgren M; Banerjee R Loss of allostery and coenzyme B<sub>12</sub> delivery by a pathogenic mutation in adenosyltransferase. *Biochemistry* 2011, 50 (25), 5790–5798. DOI: 10.1021/bi2006306. [PubMed: 21604717]
- (12). Dobson CM; Wai T; Leclerc D; Kadir H; Narang M; Lerner-Ellis JP; Hudson TJ; Rosenblatt DS; Gravel RA Identification of the gene responsible for the *cbfB* complementation group of vitamin B<sub>12</sub>-dependent methylmalonic aciduria. *Hum Mol Genet* 2002, 11 (26), 3361–3369. [PubMed: 12471062]

- (13). Ruetz M; Campanello GC; McDevitt L; Yokom AL; Yadav PK; Watkins D; Rosenblatt DS; Ohi MD; Southworth DR; Banerjee R Allosteric Regulation of Oligomerization by a B<sub>12</sub> Trafficking G-Protein Is Corrupted in Methylmalonic Aciduria. *Cell Chem Biol* 2019, 26 (7), 960–969 e964. DOI: 10.1016/j.chembiol.2019.03.014. [PubMed: 31056463]
- (14). Mascarenhas R; Ruetz M; McDevitt L; Koutmos M; Banerjee R Mobile loop dynamics in adenosyltransferase control binding and reactivity of coenzyme B<sub>12</sub>. *Proc Natl Acad Sci U S A* 2020, 117 (48), 30412–30422. DOI: 10.1073/pnas.2007332117. [PubMed: 33199623]
- (15). Stich TA; Yamanishi M; Banerjee R; Brunold TC Spectroscopic evidence for the formation of a four-coordinate Co<sup>2+</sup> cobalamin species upon binding to the human ATP:cobalamin adenosyltransferase. *J Am Chem Soc* 2005, 127 (21), 7660–7661. [PubMed: 15913339]
- (16). Gruber K; Puffer B; Krautler B Vitamin B(12)-derivatives-enzyme cofactors and ligands of proteins and nucleic acids. *Chem Soc Rev* 2011, 40 (8), 4346–4363. [PubMed: 21687905]
- (17). Liptak MD; Fleischhacker AS; Matthews RG; Telsler J; Brunold TC Spectroscopic and computational characterization of the base-off forms of cob(II)alamin. *J Phys Chem B* 2009, 113 (15), 5245–5254. DOI: 10.1021/jp810136d. [PubMed: 19298066]
- (18). Lexa D; Saveant J-M The electrochemistry of vitamin B<sub>12</sub>. *Acc. Chem. Res.* 1983, 16, 235–243.
- (19). Park K; Mera PE; Escalante-Semerena JC; Brunold TC Kinetic and spectroscopic studies of the ATP:corrinoid adenosyltransferase PduO from *Lactobacillus reuteri*: substrate specificity and insights into the mechanism of Co(II)corrinoid reduction. *Biochemistry* 2008, 47 (34), 9007–9015. DOI: 10.1021/bi800419e. [PubMed: 18672897] Pallares IG.; Moore TC.; Escalante-Semerena JC.; Brunold TC. Spectroscopic Studies of the EutT Adenosyltransferase from *Salmonella enterica*: Mechanism of Four-Coordinate Co(II)Cbl Formation. *J Am Chem Soc* 2016, 138 (11), 3694–3704. DOI: 10.1021/jacs.5b11708. [PubMed: 26886077]
- (20). Cheng S; Bobik TA Characterization of the PduS cobalamin reductase of *Salmonella enterica* and its role in the Pdu microcompartment. *J Bacteriol* 2010, 192 (19), 5071–5080. DOI: 10.1128/JB.00575-10 From NLM Medline. [PubMed: 20656910]
- (21). Mera PE; Escalante-Semerena JC Dihydroflavin-driven adenosylation of 4-coordinate Co(II) corrinoids: are cobalamin reductases enzymes or electron transfer proteins? *J Biol Chem* 2010, 285 (5), 2911–2917. DOI: M109.059485 [pii] 10.1074/jbc.M109.059485. [PubMed: 19933577]
- (22). Olteanu H; Wolthers KR; Munro AW; Scrutton NS; Banerjee R Kinetic and thermodynamic characterization of the common polymorphic variants of human methionine synthase reductase. *Biochemistry* 2004, 43 (7), 1988–1997. DOI: 10.1021/bi035910i. [PubMed: 14967039] Wolthers KR.; Basran J.; Munro AW.; Scrutton NS. Molecular dissection of human methionine synthase reductase: determination of the flavin redox potentials in full-length enzyme and isolated flavin-binding domains. *Biochemistry* 2003, 42, 3911–3920. [PubMed: 12667082]
- (23). Leclerc D; Wilson A; Dumas R; Gafuik C; Song D; Watkins D; Heng HH; Rommens JM; Scherer SW; Rosenblatt DS; and Gravel RA Cloning and mapping of a cDNA for methionine synthase reductase, a flavoprotein defective in patients with homocystinuria. *Proc Natl Acad Sci U S A* 1998, 95 (6), 3059–3064. [PubMed: 9501215]
- (24). Porter TD; Kasper CB NADPH-cytochrome P-450 oxidoreductase: flavin mononucleotide and flavin adenine dinucleotide domains evolved from different flavoproteins. *Biochemistry* 1986, 25, 1682–1687. [PubMed: 3085707]
- (25). Schulz V; Basu S; Freibert SA; Webert H; Boss L; Muhlenhoff U; Pierrel F; Essen LO; Warui DM; Booker SJ; Stehling O; and Lill R Functional spectrum and specificity of mitochondrial ferredoxins FDX1 and FDX2. *Nat Chem Biol* 2023, 19 (2), 206–217. DOI: 10.1038/s41589-022-01159-4 From NLM Medline. [PubMed: 36280795]

### Synopsis

This study reports the first experimental determination of the redox potential of 4-coordinate cob(II)alamin ( $-325 \pm 9$  mV), which was achieved by stabilizing cob(I)alamin on the R190H clinical variant of human ATP:cob(I)alamin adenosyltransferase (MMAB), which decreases the rate of the adenosylation reaction. The study also reports that mitochondrial adrenodoxin is an electron donor to MMAB. Loss of coordination control in select patient variants of MMAB results in their inability to synthesize 5'-deoxyadenosylcobalamin



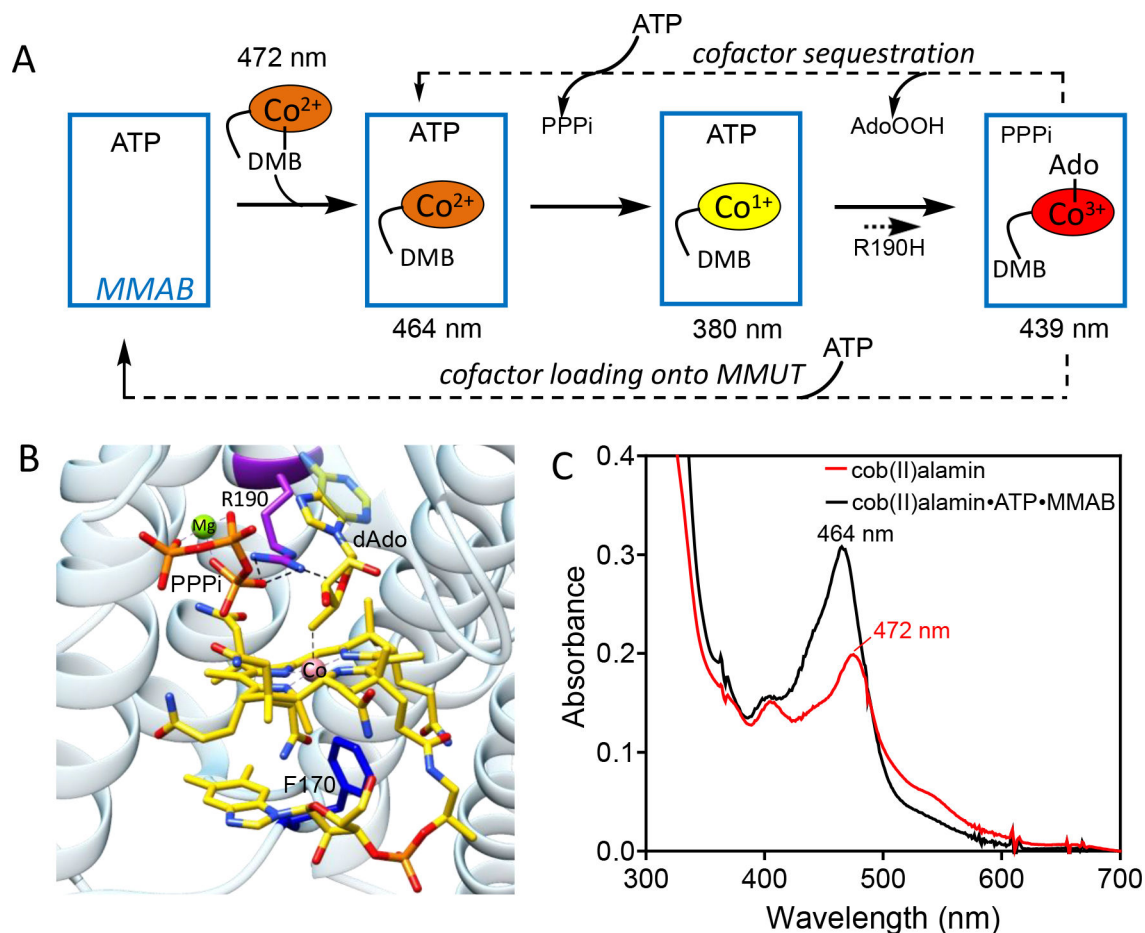


**Figure 1. AdoCbl synthesis by ATP:cob(I)alamin adenosyltransferase (MMAB).**

(A) MMAB functions in AdoCbl synthesis, transfer and sequestration. The one-electron reduction of cob(II)alamin followed by rapid adenosylation leads to AdoCbl without accumulation of the cob(I)alamin intermediate. In the presence of MMUT, AdoCbl is loaded directly onto it. In the absence of MMUT, the Co-carbon bond undergoes homolytic scission leading to sequestration of cob(II)alamin on MMAB and elimination of 5'-hydroperoxyadenosine (AdoOOH). (B) Close-up of the active site of MMAB (PDB:6D5X) with PPi (orange, stick) and AdoCbl (stick, gold). Coordination of  $O_2$  to the cobalt at the lower axial position is precluded by the non-coordinating Phe-170 (stick, blue) residue. (C) Binding of free cob(II)alamin (20  $\mu$ M in Buffer A, red) to MMAB (20  $\mu$ M, black) leads to conversion from a 5-c to 4-c state as signalled by the blue shift from 472 to 464 nm.



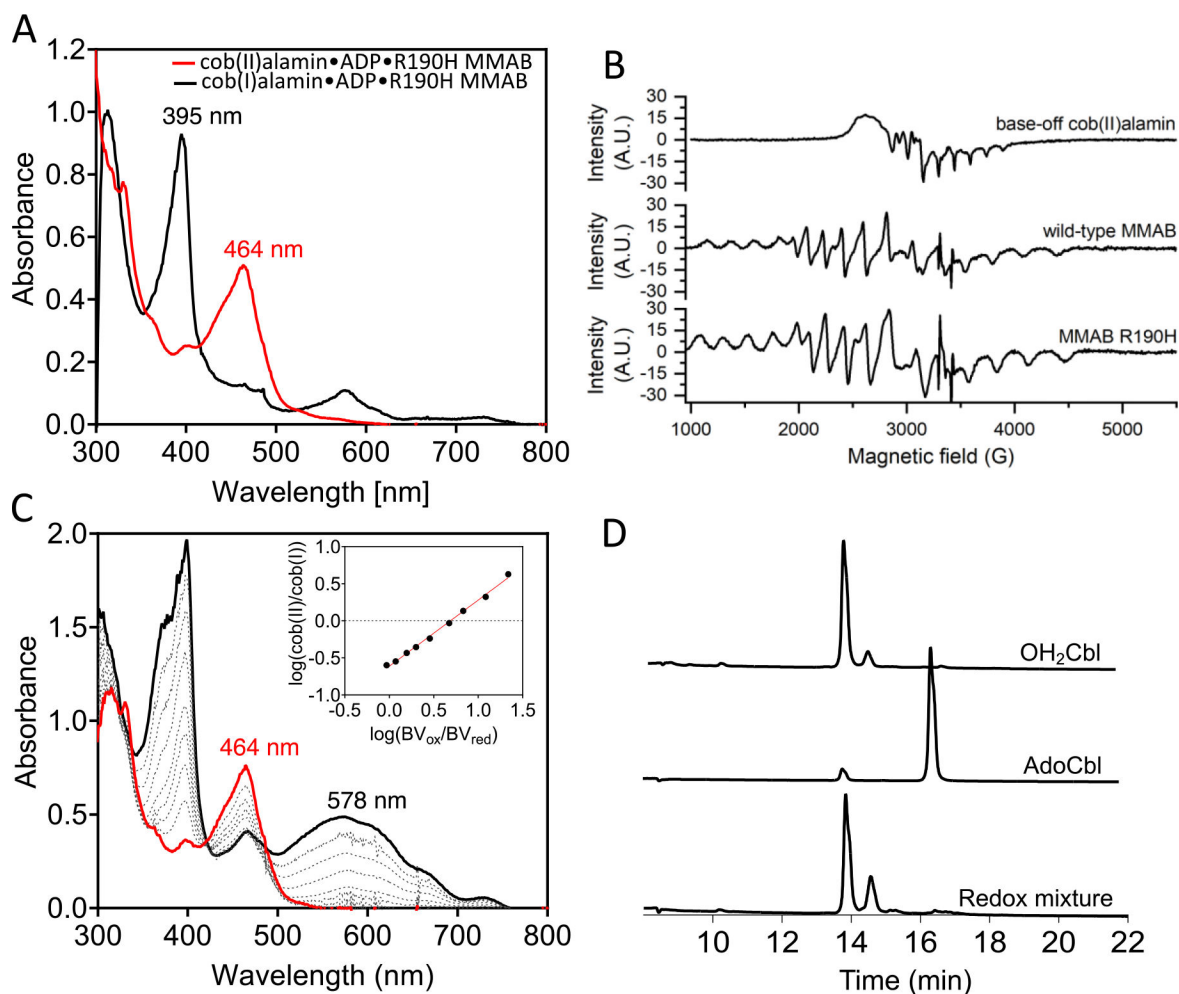


**Figure 2. Redox titration of 4-c cob(II)alamin bound to MMAB.**

(A) The one-electron reduction of cob(II)alamin (40  $\mu$ M) bound to R190H MMAB in the presence of 5 mM ADP (red) leads to accumulation of cob(I)alamin (black). (B) Comparison of the EPR spectrum of free 5-c (100  $\mu$ M) and MMAB-bound 4-c cob(II)alamin (100  $\mu$ M) indicates that the cofactor bound to the R190H variant is in the 4-c state. The principle g-values for the wild-type MMAB ( $g_x=3.342$ ,  $g_y=2.485$ ,  $g_z=1.797$ ) and R190H variant ( $g_x=3.436$ ,  $g_y=2.441$ ,  $g_z=1.768$ ) are comparable. (C) Redox titration of cob(II)alamin-bound R190H MMAB (40  $\mu$ M in Buffer A) in the presence of 5 mM ATP (red) and increasing concentrations of benzyl viologen leads to the establishment of redox equilibria. *Inset*. Nernst analysis of the titration data. (D) HPLC analysis of the titration mixture in C reveals that AdoCbl is not synthesized during the time course of the redox titration.

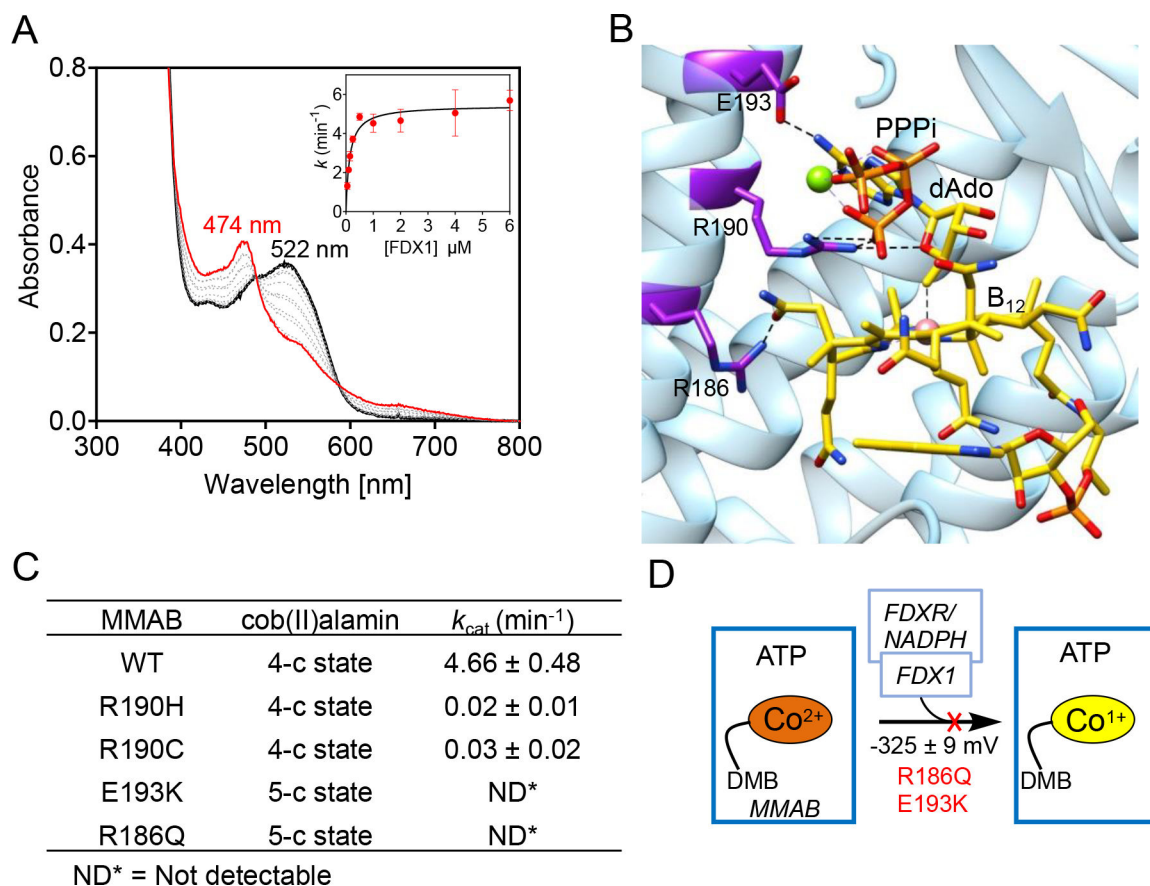


**Figure 3. FDX1 supports NADPH-dependent AdoCbl synthesis by MMAB.**

(A) NADPH-dependent FDXR/FDX1 (4  $\mu\text{M}$  each) can reduce cob(II)alamin (40  $\mu\text{M}$ , red) bound to MMAB (1  $\mu\text{M}$ ) for AdoCbl (black) synthesis. The reaction was conducted in Buffer A with 500  $\mu\text{M}$  NADPH. *Inset.* Dependence of the AdoCbl synthesis rate on FDX1 yields a  $K_M$  of  $135 \pm 24$  nM with MMAB for electron transfer. (B) Location of clinical variants used in this study, in the MMAB structure. (C) FDX1-dependent AdoCbl synthesis reveals differences in activity between wild-type and clinical variants of MMAB and a correlation with the cob(II)alamin coordination state. (D) Scheme showing that the R186Q and E193K variants impair FDX1-dependent AdoCbl synthesis by MMAB, which is correlated with methylmalonic aciduria.